



OPEN ACCESS

EDITED BY

Sami H. Mahmood,
The University of Jordan, Jordan

REVIEWED BY

Shihui Yu,
Tianjin University, China
Serhat Koçyiğit,
Bingöl University, Türkiye
Xp Jia,
Jilin University, China

*CORRESPONDENCE

Adil Alshoaibi,
✉ adshoaibi@kfupmu.edu.sa

SPECIALTY SECTION

This article was submitted to
Ceramics and Glass,
a section of the journal
Frontiers in Materials

RECEIVED 27 July 2022

ACCEPTED 24 February 2023

PUBLISHED 07 March 2023

CITATION

Alshoaibi A, Hussain F, Mohsin F, Alnaim N
and Almulhem N (2023), Different
concentrations of Ti^{4+} as a donor and
electronic properties of $Bi_{2-x}Ti_xO_3$.
Front. Mater. 10:1004889.
doi: 10.3389/fmats.2023.1004889

COPYRIGHT

© 2023 Alshoaibi, Hussain, Mohsin,
Alnaim and Almulhem. This is an open-
access article distributed under the terms
of the [Creative Commons Attribution
License \(CC BY\)](https://creativecommons.org/licenses/by/4.0/). The use, distribution or
reproduction in other forums is
permitted, provided the original author(s)
and the copyright owner(s) are credited
and that the original publication in this
journal is cited, in accordance with
accepted academic practice. No use,
distribution or reproduction is permitted
which does not comply with these terms.

Different concentrations of Ti^{4+} as a donor and electronic properties of $Bi_{2-x}Ti_xO_3$

Adil Alshoaibi^{1*}, Fayaz Hussain², Fatima Mohsin², Nisrin Alnaim¹
and Najla Almulhem¹

¹Department of Physics, College of Science, King Faisal University, Al Ahsa, Saudi Arabia, ²Department of Materials Engineering, NED University of Engineering and Technology, Karachi, Pakistan

$Bi_{(2-x)}Ti_xO_3$ ($x = 0, 0.01, 0.03$ & 0.05) (BO-xT) ceramics are prepared by conventional solid-state route followed by low sintering temperatures. X-ray diffraction analyses show the presence of the monoclinic phase of Bi_2O_3 . The electrical conductivities at room temperature concerning the frequency (ranging from 25 kHz to 5 MHz) and Seebeck Coefficient ranging from 50°C to 400°C were measured. With an increase in Ti (dopant) content, the conductivity and Seebeck Coefficient increased with the temperature increment. The BO-0.03T has the highest Seebeck value (47 $\mu V/^\circ C$), which shows a higher carrier concentration. In terms of electrical conductivities, the BO-0.05T ceramic shows the maximum electrical conductivity, i.e. $2.0 \times 10^{-9} \mu S/m$ as compared to other samples, which exhibit the presence of free electrons. Moreover, relative permittivity (dielectric constant) and dielectric loss are also measured concerning the frequency at room temperature to investigate the dielectric behaviour of the ceramics. This low-temperature sintering ceramics will open new applications in the domain of electronic materials.

KEYWORDS

solid-state synthesis, low-sintering-oxides, bismuth titanate, thermoelectric, dielectric properties

Introduction

The management of waste heat and energy efficiency in current technology is both challenging and of major concern. Thermoelectric materials, especially oxides, due to their non-toxic operation, no moving part or chemical reaction, negligible greenhouse gasses, potential scalability, and sustainability, are the most promising materials which convert heat to electricity and *vice versa* to overcome these obstacles (Petsagkourakis et al., 2018; Jia et al., 2021).

Many studies have reported that high-performance thermoelectric materials, can be described by figure of merit [i.e., $zT = (S^2\sigma/\kappa)T$, where S , σ , κ and T are Seebeck coefficient, electrical resistivity, thermal conductivity, and absolute temperature, respectively.], >2.0 for several materials in bulk form (Li et al., 2017). Since, all the factors of zT are interrelated to carrier concentration, it is demanding to optimize the power factor ($S^2\sigma$) and thermal conductivity (κ) (Han et al., 2014; Li et al., 2017; Petsagkourakis et al., 2018). Thus, several kinds of research have been carried out using different techniques, like; point defect engineering, structural designs and entropy engineering, and band engineering, to decouple these factors (Li et al., 2022). Nano-crystallization and low-dimensional processing of thermoelectric materials have proved to be important factors for high

thermoelectric performance since it helps to increase the density of state and phonon scattering that lead to an increase in the Seebeck coefficient and electric conductivity respectively while maintaining thermal conductivity (Li et al., 2022; Yang et al., 2022). However, the measurement error in the figure of merit that has been reported is of major concern due to the multiple transferring of samples during testing as it affects the intrinsic physical properties (Han et al., 2014; Han et al., 2022; Li et al., 2022; Yang et al., 2022).

So far, Bi_2O_3 with TiO_2 has been studied for its electron-conducting properties, photo-oxidative & sensing capabilities (Chadwick and Francklin, 1993; Gao et al., 2019). Bi_2O_3 is of high-mobility intrinsic p-type semiconductor that can be used as an electron donor to TiO_2 (Singla and Singh, 2014; Huang et al., 2017). δ -phase of Bi_2O_3 exhibits the highest ionic conductivity and is reported to have a conductivity of 1 S Cm^{-1} between 600°C – 800°C (Singla et al., 2012). This phase is thermally stable in the temperature range of 730°C – 825°C (Singla et al., 2012). Because of the highly volatile nature of Bi ions, it could weaken the electrical properties of ceramic and thus, its usage in various applications. The enhancement of conductivity by stabilizing δ - Bi_2O_3 at medium and low temperatures depends on the appropriate doping. This could be achieved by substitution of either isovalent or aliovalent suitable metal dopant cation. In 1990, the first successful approach for high-temperature conducting disorder phase stabilization by partial substitution of vanadium with copper was reported by Abraham et al. The perovskite-related crystal structure leads to higher ionic conductivity than parent compounds due to rapid oxygen-ion conduction. Moreover, doped Bi_2O_3 exhibits relatively low sintering temperatures with remarkable dielectric properties (Singla et al., 2012; Huang et al., 2017). Oxygen vacancies play an important role to decide the dielectric properties of these systems (Singla et al., 2012; Singla and Singh, 2013; Gao et al., 2019). Many other functional materials such as SrTiO_3 , ZnO , SnO , etc., have been investigated as good candidates for thermoelectric applications (Shi et al., 2020). Therefore, TE materials have received considerable attention from researchers. However, the thermoelectric effect in Bi_2O_3 as a substrate is a relatively less studied area, and thus it would be fascinating to explore the thermoelectric properties of Bi_2O_3 .

Due to its profound stability and flexibility in terms of structure accommodating most of the periodic table, the oxide perovskite facilitates the broad selection and adjustment of material properties. The achieved exceptional structural properties can be used in a variety of applications such as photovoltaic electrodes, superconductors, multiferroics, catalysts, batteries, resistive switches, and sensing materials. Along with their successful application in optoelectronic, piezoelectric and dielectric, halide perovskite has proved potential candidate for thermoelectric applications with a high Seebeck Coefficient and ultra-low thermal conductivity. Several reports show that the inorganic materials including; Skutterudites, PbTe , SnSe , Bi_2Te_3 , clathrate phases, and oxide perovskite have efficient thermoelectric properties in different temperature ranges. HPs including perovskite with different dimensions or ion compositions are reported to have high Seebeck coefficient and ultra-low thermal conductivity that are intrinsically favourable for thermoelectric materials. These factors have paved the way for their application in the thermoelectric field. However, reported relatively small electric conductivity has restricted the power factor (PF) and

dimensionless figure of merit (ZT) of HPs. Various experimental works have been done to optimize the electrical conductivity of HPs by adopting techniques like enhancing charge carrier concentration and reducing the charge transport barrier. Hence, balancing the correlated parameters is still one of the major concerns of HPs.

This study aims to synthesize thermoelectric materials with less energy consumption during thermal treatment. For this, a set of $\text{Bi}_{(2-x)}\text{Ti}_x\text{O}_3$ ($x = 0, 0.01, 0.03$ & 0.05) ceramics have been prepared to investigate the effect of TiO_2 doping on Bi_2O_3 . The as-prepared samples were characterized and tested to study the thermoelectric and dielectric properties.

Experimental procedure

The preparation of ceramic compounds with the chemical formula $\text{Bi}_{(2-x)}\text{Ti}_x\text{O}_3$ ($x = 0, 0.01, 0.03$ & 0.05) was carried out *via* the conventional solid-state synthetic method. The oxides Bi_2O_3 and TiO_2 were used as precursors for the synthesis of present compounds. The synthesis involved batching raw materials stoichiometrically and grounded together in porcelain mortar in a methanol medium. The grounded powders were then calcined at 700°C for 3 h followed by further mixing and rigorous grinding and finally sieving to achieve homogeneity. The green powders were then mixed with polyvinyl alcohol (PVA) binder and pelletized using a YLG Powder Pressing machine with 0.5 MPa into a die of 12.7 mm diameter. The pellets were sintered at 750°C for 2.5 h.

The compounds, thus formed, were named BO (i.e., Bi_2O_3), BO-0.01T (i.e., $\text{Bi}_{1.99}\text{Ti}_{0.01}\text{O}_3$), BO-0.03T (i.e., $\text{Bi}_{1.97}\text{Ti}_{0.03}\text{O}_3$), and BO-0.05T (i.e., $\text{Bi}_{1.95}\text{Ti}_{0.05}\text{O}_3$), considering different dopant concentrations, were characterized and used to carry out further studies. X-ray diffraction pattern of $\text{Bi}_{(2-x)}\text{Ti}_x\text{O}_3$ ($x = 0, 0.01, 0.03$ & 0.05) were obtained using Cu-K α radiation on x-ray diffractometer (PANalytical, X'Pert Pro, made in Netherland) within scanning range of 10° – 80° . For conductivity, the silver paste was applied to both sides of the pellets and cured at 400°C for 3 h. The samples were evaluated using a Tonghui TH2826 LCR meter to measure the dielectric losses, electrical permittivity, and electrical conductivity within a frequency range from 25 to 1 MHz at room temperature.

The pellets of each composition were stacked up to observe the relation between thermal gradient and Seebeck Coefficient by using a setup containing a KEITHLEY 2612A Nano-voltmeter, hot plate, and digital meter in the temperature range of 50°C – 400°C . The stacking was done by coating the silver adhesive to produce a greater thermal gradient and minimize the contact resistance.

Results and discussion

The XRD pattern of air-sintered samples at 750°C for 2.5 h with different concentrations of dopant (i.e., TiO_2) at room temperature with the scanning rate of 0.02/min is shown in Figure 1. $\text{Bi}_{(2-x)}\text{Ti}_x\text{O}_3$ ($x = 0, 0.01, 0.03$ & 0.05) ceramics matched with the standard data ICDD exhibit monoclinic Bi_2O_3 crystal phase (PDF 001-076-1730 & PDF 003-065-2366) with a space group of P21/c for all four prepared samples. While demonstrating the phase purity of Bi_2O_3 , no such impurities were detected. According to reports, Bi_2O_3 has six different polymorphs, namely; monoclinic, triclinic, tetragonal,

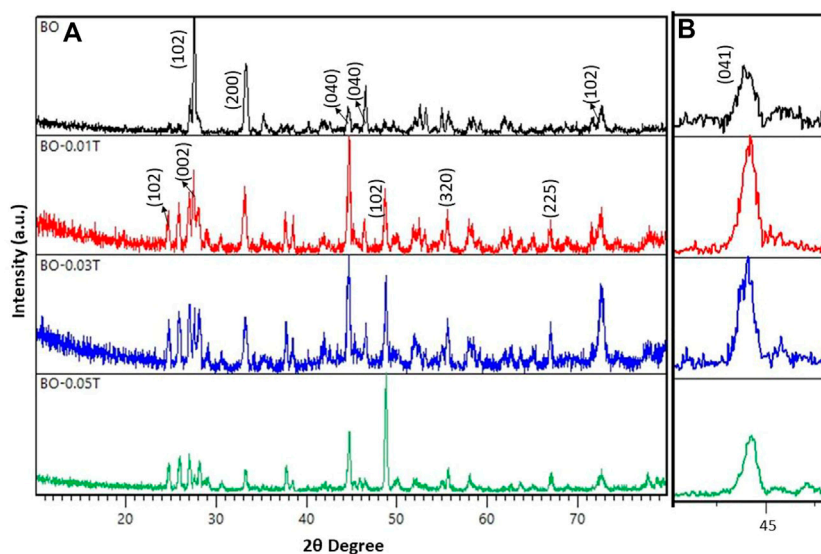


FIGURE 1
(A) X-ray diffraction patterns of sintered pellets at 750°C (B) enlarged 45° peak.

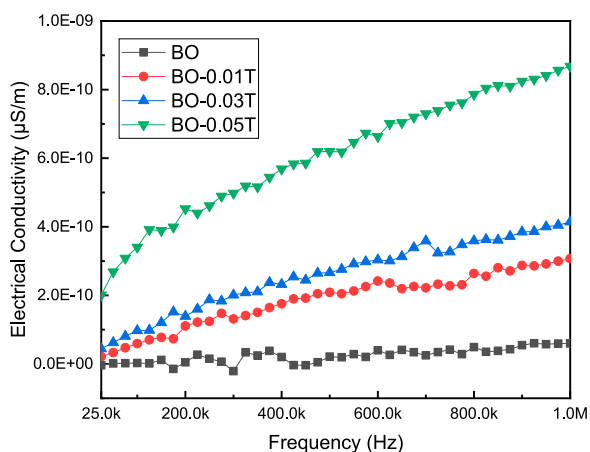


FIGURE 2
Electrical Conductivities of sintered pellets at 750°C as a function of frequency.

orthorhombic, body-centred cubic, and face-centred cubic, in which the monoclinic structure of Bi_2O_3 is favourable for superconductivity at high temperatures (Chadwick and Francklin, 1993; Singla and Singh, 2014). The secondary phase peaks of TiO_2 are detected in the doped samples. The sharp peaks with high intensity indicate that materials are well crystallized. The high-intensity peaks observed at 25°, 26°, 48.9°, 56°, and 67° were respectively indexed as (102), (002), (102), (320), and (225) planes of monocline Bi_2O_3 in doped samples (i.e., BO-0.01T, BO-0.03T, & BO-0.05T). With an increase in Ti content, the intensity of diffraction peaks at 45° gradually increased, indicating the continuous improvement of the crystallinity of Bi_2O_3 . Almost all the peak positions for different Ti concentrations are the same and

no peak shifts were observed, this could attribute to the same lattice parameter (Singla and Singh, 2014; Rini and Restiana, 2019). The results showed the successful synthesis of the bismuth titanium oxide compound. The relative densities of all sintered pellets were over 90%, which is dense enough for thermoelectric studies.

The frequency dependence of electrical conductivity at room temperature is shown in Figure 2. The frequency spectrum ranging from 25 kHz to 1 MHz shows an increase in electrical conductivity in all compositions concerning the frequency indicating semiconducting behaviour (Hong et al., 2019). The conductivity results due to the absence of Bi^{3+} ions that produced the lattice defect or the excess of oxygen. The electrical conductivity has improved by doping Ti^{4+} ions (Mansfield and Mansfield, 1946). Among all compositions, BO-0.05T -the highly doped ceramic-shows the highest electrical conductivity, i.e., $2.0 \times 10^{-9} \mu\text{S/m}$ which exhibits the presence of free hole carriers and porosities (Li et al., 2000; Park et al., 2009; Koçyiğit et al., 2020). It can be observed that with the increase in dopant (Ti) concentration, the conductivity of the samples has also increased which is favourable for the high thermoelectric performance, i.e., figure of merit (ZT) (Koumoto et al., 2013; Shi et al., 2020; Han et al., 2022).

The measured Seebeck Coefficient versus average temperature in the range of 50 °C–400 °C is shown in Figure 3. For the Seebeck Coefficient (S) measurement, a thermal gradient of approximately 50 °C was obtained for all samples. The Seebeck Coefficient of all samples increases with increasing temperature as according to the theory of semiconductors with the electronic structures of broader bands, the carrier mobility is higher with large values of the Seebeck coefficient and electrical conductivity. The S values for almost all samples were around $13 \mu\text{V}/^\circ\text{C}$ at 50°C which considerably improved over the wide range of temperatures, which could be ascribed to an increase in carrier density at high temperatures as the increasing Ti content for $\geq 150^\circ\text{C}$ (Koumoto et al., 2013; Zuo et al., 2018). It can be observed from the graph that the Seebeck Coefficient

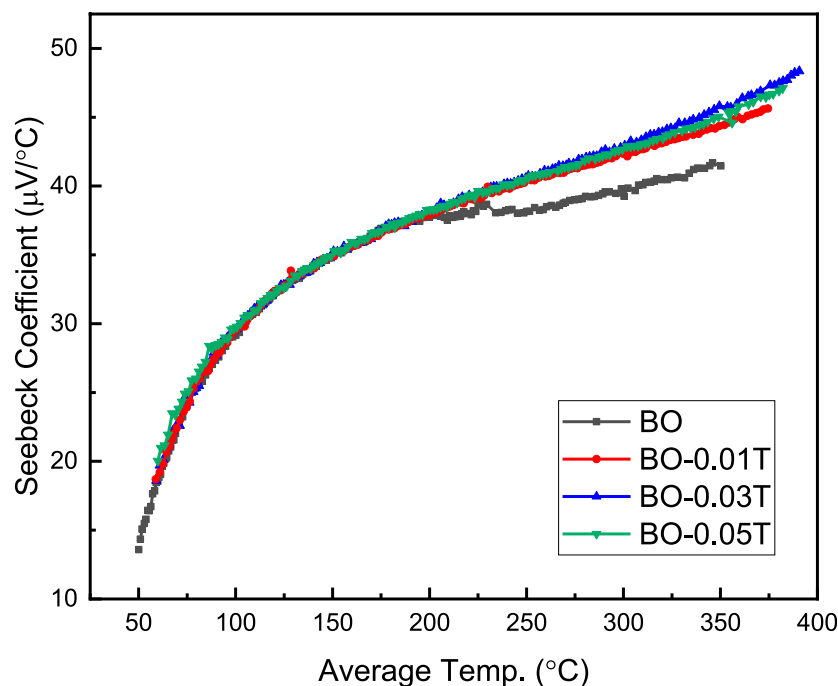


FIGURE 3
Temperature dependence on Seebeck Coefficient of stack pellets sintered at 750°C.

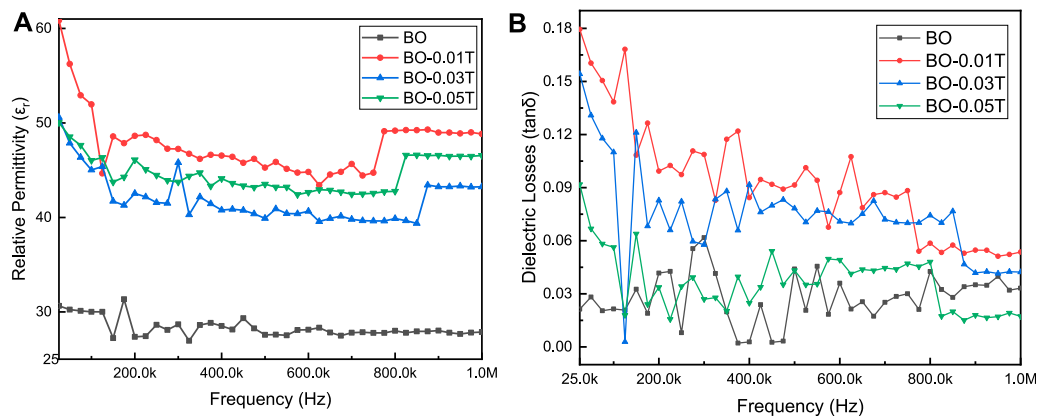


FIGURE 4
(A) Relative permittivity and (B) Tangent loss of sintered pellets at 750°C as a function of frequency at room temperature.

of all doped samples has an almost similar trend till 300°C, however, the Seebeck coefficient of pure ceramic (BO) has shown a slight decrease after 200°C as compared to other doped samples. The samples show enhancement in electrical conductivity and the Seebeck Coefficient after Ti doping which could lead to high power factor values as compared to the un-doped sample (Koçyiğit et al., 2014; Koçyiğit et al., 2019; Ghosh et al., 2020). Among all compositions, as-prepared samples BO-0.03T has the highest Seebeck value, i.e., 47 $\mu\text{V}/^\circ\text{C}$ which shows the presence of a higher carrier concentration (Terasaki, 2011), while BO-0.03T has the second-highest electrical conductivity value. The power factor,

i.e., $S^2\sigma$ of BO-0.03T ceramic could contribute to a greater figure of merit or thermoelectric properties (Martin et al., 2010; Dorey, 2012).

The dielectric properties of sintered samples at room temperature were also studied. Figures 4A, B show the dielectric constant (relative permittivity) and tangent loss ($\tan\delta$) as a function of frequency in the range of 25 kHz to 1 MHz respectively. The dielectric constant values continuously decrease and increase with an increase in frequency due to the change of polarization mechanism phenomenon (Martin et al., 2010; Terasaki, 2011; Dorey, 2012; Gao et al., 2019; Ghosh et al., 2020). This change originates due to the activation of one or more sources from

electronic, ionic, atomic, dipolar, and space charge polarization at different frequency levels (Dorey, 2012; Santos et al., 2013). At the low-frequency level, the dielectric constant decrease with an increase in temperature due to the abatement in space charge polarization effect (Dorey, 2012; Singla et al., 2012; Singla and Singh, 2013; Rayssi et al., 2018; Gao et al., 2019). The doping of Ti^{4+} in Bi_2O_3 considerably increased the dielectric constant as defects, and impurity also has effects on ϵ_r . BO-0.01T shows the highest permittivity values while the pristine BO has relatively lesser values among the four compositions. It may attribute to high oxygen vacancies and defects (Gao et al., 2019). It can be observed from the graph (Figure 4A) that all samples remain stable with a very slight change in relative permittivity for a broader range of frequencies. Nonetheless, it could be due to the resonance of ionic or electronic polarization (Dorey, 2012; Singla and Singh, 2013). The loss tangent represents the energy losses that occur due to the polarization shifts when the external field is applied and is related to the relaxation process in dielectric materials (Dorey, 2012; Academia, 2022). The losses, in general, originate due to one of these three factors; DC conduction, interfacial polarization contribution, and dipole loss (Rayssi et al., 2018; Gao et al., 2019; Academia, 2022). The tangent losses in all samples at room temperature vary largely with increasing frequency; this may be due to the reordering of interfacial dipoles under the applied field. The losses become relatively less with an increase in frequency. Doped samples have relatively higher losses than the un-doped sample, this may result because of impurities and defects such as oxygen vacancies and these defects could enhance the leakage current that leads to the increment in the conductive loss (Singla and Singh, 2013; Rayssi et al., 2018; Gao et al., 2019). At high frequency, BO-0.01T has maximum losses ~ of 18% and un-doped BO shows minimum losses ~ of 4%. This could be due to localized accumulation of charge and free electrons under the applied electrical field (Dorey, 2012).

Conclusion

In this work, the $Bi_{(2-x)}Ti_xO_3$ ($x = 0, 0.01, 0.03$ & 0.05) ceramics (>90% dense) were prepared by conventional solid-state route followed by low-temperature sintering ($750^\circ C$). The prepared samples were characterized, and their thermoelectric and dielectric properties were investigated. The Ti dopant has shown a remarkable effect on Bi_2O_3 . With an increase in dopant concentration, the electrical conductivity and Seebeck Coefficient increased which could contribute to a greater power factor ($S^2\sigma$) and thermoelectric properties. Furthermore, the dielectric constant and tangent losses increase with an increase in dopant concentration at room temperature. At high frequency, BO

shows the minimum losses, while BO-1T exhibits the higher permittivity among all compositions.

Data availability statement

The original contributions presented in the study are included in the article/supplementary material, further inquiries can be directed to the corresponding author.

Author contributions

AA, conceptualization, methodology, writing—review and editing. FH, conceptualization, methodology, data curation, writing—original draft, visualization, investigation, supervision. FM, data curation, writing—original draft, visualization, investigation. NiA, writing—review and editing. NaA, writing—review and editing.

Funding

All authors very thankful to the Department of Materials Engineering, NED University of Engineering & Technology, Karachi, Pakistan; for experimental work and lab support to finish this work with collaboration. This work was supported through the Annual Funding track by the Deanship of Scientific Research, Vice Presidency for Graduate Studies and Scientific Research, King Faisal University, Saudi Arabia (Project No. AN000484).

Conflict of interest

The authors declare that the research was conducted in the absence of any commercial or financial relationships that could be construed as a potential conflict of interest.

Publisher's note

All claims expressed in this article are solely those of the authors and do not necessarily represent those of their affiliated organizations, or those of the publisher, the editors and the reviewers. Any product that may be evaluated in this article, or claim that may be made by its manufacturer, is not guaranteed or endorsed by the publisher.

References

- Academia (2022). CHE 697_Research project 2_Thesis full Report_Mohd wishal | wishal kurnia - Academia.edu. https://www.academia.edu/50941027/CHE_697_Research_Project_2_Thesis_Full_Report_Mohd_Wishal.
- Chadwick, A. v., and Francklin, A. J. (1993). Thermoelectric power studies of bismuth oxide and mixed oxides based on bismuth oxide. *Philosophical Mag. A Phys. Condens. Matter, Struct. Defects Mech. Prop.* 68, 787–797. doi:10.1080/01418619308213997
- Dorey, R. (2012). "Microstructure–property relationships," in *Ceramic thick films for MEMS and microdevices* (Amsterdam, Netherlands: Elsevier). 85–112.
- Gao, R., Qin, X., Wu, H., Xu, R., Liu, L., Wang, Z., et al. (2019). Effect of Ti doping on the dielectric, ferroelectric and magnetic properties of $Bi_{0.86}La_{0.08}Sm_{0.14}FeO_3$ ceramics. *Mater. Res. Express* 6, 106317. doi:10.1088/2053-1591/ab3fee
- Ghosh, S., Harish, S., Ohtaki, M., and Saha, B. B. (2020). Thermoelectric figure of merit enhancement in cement composites with graphene and transition metal oxides. *Mater. Today Energy* 18, 100492. doi:10.1016/j.mtener.2020.100492
- Han, C., Li, Z., and Dou, S. (2014). Recent progress in thermoelectric materials. *Chin. Sci. Bull.* 59, 2073–2091. doi:10.1007/s11434-014-0237-2

- Han, Z., Li, J. W., Jiang, F., Xia, J., Zhang, B. P., Li, J. F., et al. (2022). Room-temperature thermoelectric materials: Challenges and a new paradigm. *J. Materiomics* 8, 427–436. doi:10.1016/j.jmat.2021.07.004
- Hong, M. H., Choi, H., Kim, Y., Kim, T., Cho, H. H., Driss, Z., et al. (2019). Ti doping effects on the Seebeck coefficient and electrical conductivity of mesoporous ZnO thin film. *Mater. Chem. Phys.* 235, 121757. doi:10.1016/j.matchemphys.2019.121757
- Huang, Y., Wei, Y., Wang, J., Luo, D., Fan, L., and Wu, J. (2017). *Controllable Fabrication of Bi₂O₃/TiO₂ Heterojunction with excellent visible-light responsive photocatalytic performance*. Available at: <http://www.elsevier.com/open-access/userlicense/1.0/>.
- Jia, N., Cao, J., Tan, X. Y., Dong, J., Liu, H., Tan, C. K. I., et al. (2021). Thermoelectric materials and transport physics. *Mater. Today Phys.* 21, 100519. doi:10.1016/j.mtphys.2021.100519
- Koçyiğit, S., Aytımur, A., Çınar, E., Uslu, İ., and Akdemir, A. (2014). Boron-doped strontium-stabilized bismuth cobalt oxide thermoelectric nanocrystalline ceramic powders synthesized via electrospinning. *JOM* 66, 30–36. doi:10.1007/s11837-013-0822-x
- Koçyiğit, S., Aytımur, A., and Uslu, İ. (2020). Graphene-doped Ca_{0.9}Er_{0.1}Mn_{1.5}O_α thermoelectric nanocomposite materials: Temperature-dependent thermal and Seebeck properties. *Ceram. Int.* 46 (5), 6377–6382. doi:10.1016/j.ceramint.2019.11.115
- Koçyiğit, S., Aytımur, A., and Uslu, İ. (2019). Temperature dependent Seebeck coefficient and thermal conductivity properties of graphene undoped and doped Ca-Pr-Co oxide thermoelectric nanocomposites. *J. Vac. Sci. Technol. A Vac. Surfaces, Films* 37 (6), 061201. doi:10.1116/1.5121253
- Koumoto, K., Funahashi, R., Guilmeau, E., Miyazaki, Y., Weidenkaff, A., Wang, Y., et al. (2013). Thermoelectric ceramics for energy harvesting. *J. Am. Ceram. Soc.* 96, 1–23. doi:10.1111/jace.12076
- Li, J. F., Pan, Y., Wu, C. F., Sun, F. H., and Wei, T. R. (2017). Processing of advanced thermoelectric materials. *Sci. China Technol. Sci.* 60, 1347–1364. doi:10.1007/s11431-017-9058-8
- Li, S., Funahashi, R., Matsubara, I., Ueno, K., Sodeoka, S., and Yamada, H. (2000). Synthesis and thermoelectric properties of the new oxide materials Ca_{3-x}Bi_xCo₄O₉₊δ (0.0<x<0.75). *Chem. Mater.* 12 (8), 2424–2427. doi:10.1021/cm000132r
- Li, W., Xu, T., Ma, Z., Cheng, Y., Li, J., Jiang, Q., et al. (2022). High thermoelectric performance in p-type InSb with all-scale hierarchical architectures. *Mater. Today Energy* 29, 101091. doi:10.1016/J.MTENER.2022.101091
- Mansfield, R., and Mansfield, B. R. (1946). The electrical properties of bismuth oxide. *J. Soc. Glass Tech.* 17.
- Martin, J., Tritt, T., and Uher, C. (2010). High temperature Seebeck coefficient metrology. *J. Appl. Phys.* 108, 121101. doi:10.1063/1.3503505
- Park, J. W., Kwak, D. H., Yoon, S. H., and Choi, S. C. (2009). Thermoelectric properties of Bi, Nb co-substituted CaMnO₃ at high temperature. *J. Alloys Compd.* 487 (1–2), 550–555. doi:10.1016/j.jallcom.2009.08.012
- Petsagkourakis, I., Tybrandt, K., Crispin, X., Ohkubo, I., Satoh, N., and Mori, T. (2018). Thermoelectric materials and applications for energy harvesting power generation. *Sci. Technol. Adv. Mater.* 19, 836–862. doi:10.1080/14686996.2018.1530938
- Rayssi, C., el Kossi, S., Dhahri, J., and Khirouni, K. (2018). Frequency and temperature-dependence of dielectric permittivity and electric modulus studies of the solid solution Ca_{0.85}Er_{0.1}Ti_{1-x}Co_{4x}/3O₃ (0 ≤ x ≤ 0.1). *RSC Adv.* 8, 17139–17150. doi:10.1039/c8ra00794b
- Rini, A. S., and Restiana, S. (2019). Diffraction pattern simulation of crystal structure towards the ionic radius changes via vesta program. *J. Technomaterial Phys.* 1, 132–139. doi:10.32734/jotpv.1i12.1288
- Santos, D. J., Barbosa, L. B., Silva, R. S., and Macedo, Z. S. (2013). Fabrication and electrical characterization of translucent Bi<sub>_{b>12}TiO_{_{b>20}Ceramics. *Adv. Condens. Matter Phys.* 2013, 1–7. doi:10.1155/2013/536754}
- Shi, X. L., Zou, J., and Chen, Z. G. (2020). Advanced thermoelectric design: From materials and structures to devices. *Chem. Rev.* 120, 7399–7515. doi:10.1021/acs.chemrev.0c00026
- Singla, G., Jha, P. K., Gill, J. K., and Singh, K. (2012). Structural, thermal and electrical properties of Ti⁴⁺ substituted Bi₂O₃ solid systems. *Ceram. Int.* 38, 2065–2070. doi:10.1016/j.ceramint.2011.10.043
- Singla, G., and Singh, K. (2013). Dielectric properties of Ti substituted Bi_{2-x}Ti_xO_{3+x/2} ceramics. *Ceram. Int.* 39, 1785–1792. doi:10.1016/j.ceramint.2012.08.025
- Singla, G., and Singh, K. (2014). Effect of TiO₂ on the photocatalytic properties of bismuth oxide. *Environ. Technol. (United Kingdom)* 35, 1520–1524. doi:10.1080/09593330.2013.871583
- Terasaki, I. (2011). High-temperature oxide thermoelectrics. *J. Appl. Phys.* 110, 053705. doi:10.1063/1.3626459
- Yang, X., Wang, C., Lu, R., Shen, Y., Zhao, H., Li, J., et al. (2022). Progress in measurement of thermoelectric properties of micro/nano thermoelectric materials: A critical review. *Nano Energy* 101, 107553. doi:10.1016/j.nanoen.2022.107553
- Zuo, G., Kemerink, M., Wang, E., and Campoy-Quiles, M. (2018). *Doping and density of states engineering for organic thermoelectrics*. Linköping, Sweden: Complex Materials and Devices Department of Physics, Chemistry and Biology (IFM) Linköping University, SE-581 83.